miR-483 promotes the development of colorectal cancer by inhibiting the expression level of EI24

WEI ZHOU[1*], WANLI YANG[1*], JING YANG[2*], HAIJUN ZHU[3*], LILI DUAN[1], XIAOQIAN WANG[1],
YIDING LI[1], LIAORAN NIU[1], SHUAO XIAO[1], RUI ZHANG[1], JIANJUN YANG[1] and LIU HONG[1]

[1]Department of Gastrointestinal Surgery, Xijing Hospital of Digestive Diseases, [2]Department of Emergency,
Xijing Hospital, The Fourth Military Medical University, Xi'an, Shaanxi 710032;
[3]Department of General Surgery, Xi'an Central Hospital, Xi'an, Shaanxi 710003, P.R. China

Abstract. MicroRNAs (miRs) serve an important role in cell differentiation, proliferation and apoptosis by negatively regulating gene expression at the transcriptional or post-transcriptional level. EI24 autophagy associated transmembrane protein (EI24) is a tumor suppressor gene that serves an important role in the occurrence and development of digestive system tumors. However, little is known regarding the relationship between EI24 and the prognosis of patients with colorectal cancer (CRC). Our previous study confirmed EI24 as the target molecule of miR-483, using reporter gene detection. Thus, the aim of the present study was to elucidate the effect of the abnormal expression of miR-483 on the malignant phenotype of CRC through a series of cell function experiments and nude mice tumorigenicity experiments, and to determine the expression level of EI24, a downstream target gene of miR-483, in CRC and its relationship with patient prognosis. In CRC tissues and cells, the expression level of miR-483 was upregulated, while the expression level of EI24 was downregulated. Cell function tests such as MTT assay, cell cycle assay, colony formation assay, Migration and invasion assays and nude mice tumorigenicity experiments demonstrated that the overexpression of miR-483 promoted the proliferation, invasion and metastasis of CRC. Moreover, the reverse transcription-quantitative PCR results indicated that overexpression of miR-483 inhibited the expression level of EI24. The relationship between the clinical data and immunohistochemical results from 183 patients with CRC and survival was examined. It was found that the expression level of EI24 was positively associated with the prognosis of patients. As a cancer-promoting factor, miR-483 enhances the proliferation, migration and invasion of CRC cells by reducing the expression level of EI24.

Introduction

Colorectal cancer (CRC) is the fourth most deadly cancer in the world with nearly 900,000 deaths annually, accounting for about 10% of all annually diagnosed cancers and cancer-related deaths (1). The occurrence of CRC is a multi-step process. Invasion and metastasis are the main causes of morbidity and mortality, and ~1/3 of patients with CRC eventually develop metastatic disease (2). Therefore, early diagnosis can directly affect or even determine the survival time of patients with CRC. The pathogenesis of CRC is complex, involving the regulation of numerous molecular pathways including Wnt/β-catenin, p53, TGF-β/SMAD, NF-κB and Notch signaling pathways (3). Thus, studies into the molecular mechanisms of CRC will aid in the development of novel molecular diagnostic tools and targeted treatment methods, and thus improve the survival of patients.

MicroRNAs (miRNAs/miRs) are a large class of highly conserved endogenous non-coding single-stranded small RNAs, 18-25 nucleotides in length (4). At present, >28,600 miRNAs have been identified, of which >2,600 mature miRNAs have been found in humans (5). miRNAs bind to the 3'untranslated region of target gene mRNA through incomplete base pairing and form an RNA-induced silencing complex, which promotes the degradation of RNA or inhibits the translation of proteins, thereby regulating the expression of the downstream target genes (6). Furthermore, miRNAs have been found to regulate gene expression in numerous biological processes in cells, including proliferation, differentiation, metabolism and apoptosis (7).

The gene of miR-483 is located in the second intron region of insulin-like growth factor receptor 2 on chromosome 11 (8). Since it was first cloned in the human embryonic liver in 2005, researchers have identified that the expression pattern of

miR-483 is inconsistent among different types of tumors. For instance, large number of studies have reported that miR-483 was not only involved in the occurrence of relatively benign diseases, such as type 2 diabetes, osteoarthritis, ischemic heart disease and polycystic ovary syndrome, but was also involved in the occurrence of malignant tumors, including nephroblastoma, lung cancer, adrenocortical carcinoma and numerous digestive system tumors (9-16). Moreover, miR-483 serves a role in multiple biological functions of tumor cells, acting on target mRNAs that are closely associated with the occurrence and development of tumors (17).

EI24 autophagy associated transmembrane protein (EI24) is an early, rapidly induced gene involved in p53-mediated apoptosis (18). Furthermore, it serves an important role in inhibiting cell proliferation and activating autophagy, as well as exerts tumor-suppressive activity (19). The human EI24 gene is located on chromosome 11q23, where heterozygote deficiency occurs in a variety of malignant tumors, leading to the decrease or disappearance of its anti-cancer function (20). Abnormalities in EI24 expression are closely associated with the occurrence and progression of tumors (21-23). In addition, our previous study confirmed EI24 as the target molecule of miR-483, using reporter gene detection (24).

The present study aimed to investigate the effects of miR-483 and EI24 on the malignant phenotype of CRC, the regulation of EI24 expression by miR-483 and its significance in CRC.

Materials and methods

Cell culture and clinical samples. The normal colorectal epithelial cell line, NCM460, and the CRC cell lines, Caco-2, RKO, LoVo and HCT 116, were cultured in RPMI-1640 medium (Gibco; Thermo Fisher Scientific, Inc.) supplemented with 1% penicillin-streptomycin (HyClone; Cytiva) and 10% FBS (HyClone; Cytiva) in a cell incubator at 37°C under a humidified atmosphere of 5% CO_2.

A total of 183 cases of CRC and adjacent normal mucosa tissue specimens were collected from Xijing Hospital of The Fourth Military Medical University (age range, 24-91 years) between January 1, 2014 and December 31, 2015; the date of last complete follow-up was December 31, 2019. All specimens were diagnosed as CRC by postoperative pathological examination, and the clinical features of the specimens are presented in the Table SI. All tissue samples used in this study were immediately frozen in liquid nitrogen and stored at -80°C. The use of patient data was approved by the patient and his/her family members, and the study was approved by the Ethics Committee of Xijing Hospital, The Fourth Military Medical University (approval no. KY20203211-1). All operations were performed in accordance with the Helsinki Declaration and good clinical practice guidelines (25).

Reverse transcription-quantitative (RT-q)PCR. PCR primers and RT primers were designed and synthesized by Guangzhou RiboBio Co., Ltd., and RNA was extracted using TRIzol (Invitrogen; Thermo Fisher Scientific, Inc.) according to the manufacturer's protocols. The quality of RNA was detected via the ultraviolet absorption method. The purity of RNA was determined using 10% denaturing agarose gel electrophoresis.

Isolated RNAs were reverse transcription using the Promega M-MLV kit (cat. no. M1705; Promega Corporation) according to the manufacturer's protocols. The cDNA was used to perform RT-qPCR on LightCycler 480 Real-time PCR system(Roche, USA) using the SYBR Master Mix (cat. no. DRR041B; Takara Bio). Amplification was performed at 95°C for 30 sec, followed by 40 cycles of 95°C for 5 sec and 60°C for 30 sec. U6 was used as an endogenous control for miRNA detection, and GAPDH was used as the RT-qPCR control of EI24. The following primers were used in the study: U6 forward, 5'-CGCTTC GGCAGCACATATACTA-3' and reverse, 5'-CGCTTCACG AATTTGCGTGTCA-3'; GAPDH forward, 5'-TGACTTCAA CAGCGACACCCA-3' and reverse, 5'-CACCCTGTTGCT GTAGCCAAA-3'; and EI24 forward, 5'-AATGCACCAGCG GTTGTCTAA-3' and reverse, 5'-GATAGAGAAAAGGCA GCCACTGA-3'; miR-483 5'-AAGACGGGAGGAAAGAAG GGA-3'. The relative RNA expression level was calculated using the $2^{-\Delta\Delta Cq}$ method (26).

Cell transfection. The human CRC cell line Caco-2 was cultured in RPMI-1640 complete medium containing 1% penicillin-streptomycin (10,000 U/ml; cat. no. 15140122; Gibco; Thermo Fisher Scientific, Inc.) and 10% FBS at 37°C with 100% humidity and 5% CO_2. To generate the hsa-miR-483 lentiviral expression plasmid, the pre hsa-miR-483 sequence (GGAAAGGACGAAACACCGGCTGATGGC ACCTGCCCTTTGG) was synthesized and cloned into lentiviral expression vector GV309 (Shanghai GeneChem Co., Ltd.). A scrambled sequence (TTCTCCGAACGTGTCACGT) was created as a negative control construct. The miR-483 lentivirus (LV-miR-483) and negative control (LV-NC) virus were GFP (Green fluorescent protein)-tagged. After being confirmed by DNA sequencing, 293 cells (Cell Resource Center, Institute of Basic Medicine, Chinese Academy of Medical Sciences) were co-transfected with the vector plasmid and the packing plasmids of pHelper 1.0 and pHelper 2.0 (Shanghai GeneChem Co., Ltd.). To obtain stable lentivirus infected cell lines, Caco-2 cells were plated at 30% confluence and lentivirus vector (1x10⁹ TU/ml) containing 2 mg/ml polybrene (Shanghai GeneChem Co., Ltd.) was transfected into serum-free medium under the conditions of 37°C, 100% humidity and 5% CO_2. After 16 h, fresh complete medium was used instead of culture medium. The transfection efficiency was observed via fluorescence microscope (magnification, x100) 72 h later. After transfection with 48 h, RT-qPCR was used to verify whether the transfection was successful. miR-483 inhibitor was used to construct miR-483 low expression CRC cells. 100 pmol miR-483 inhibitor (cat. no. miR20002173-1-5; Guangzhou RiboBio Co., Ltd.) or inhibitor NC (cat. no. miR20002173-1-5; Guangzhou RiboBio Co., Ltd.) was added into 250 μl Opti-MEM (Gibco; Thermo Fisher Scientific, Inc.), 5 μl Lipofectamine 2000® (Invitrogen; Thermo Fisher Scientific, Inc.) reagent was diluted and mixed with 250 μl Opti-MEM at room temperature for 5 min. Lipofectamine® was mixed with miR-483 inhibitor or inhibitor NC at room temperature for 20 min. The complexes of inhibitor or inhibitor NC were added into Caco-2 cells respectively. The cells were incubated at 37°C, 100% humidity and 5% CO_2. After transfection for 48 h, RT-qPCR was used to verify whether the transfection was successful.

MTT assay. Logarithmic growth stage cells were inoculated into 96-well plates with 3,000 cells per well, using a micro-sample gun, and then cultured in a cell culture box under the conditions of 37˚C, 100% humidity and 5% CO_2. The following day, 20 μl sterile MTT solution (5 mg/ml; Beijing Dingguo Changsheng Biotechnology, Co., Ltd.) was added to the wells. After 4 h, the culture solution in each well was absorbed and removed. DMSO (100 μl; Sigma-Aldrich; Merck KGaA) was added to each well to dissolve the formazan particles. An oscillator was used for oscillation at 37˚C for 5 min at a frequency of 20 rpm, and the optical density value was measured at 490/570 nm using an enzyme labeling instrument.

Cell cycle assay. Cells in the logarithmic growth stage ($1x10^6$ cells/well) were resuspended in a cell suspension, centrifuged several times (room temperature, 200 x g, 5 min) and immobilized with 75% ethanol. Cells were suspended in cell staining solution containing 0.01% RNase and 0.5% propidium iodide (Shanghai Ruji Biological Technology Development Co., Ltd.) and stained at 4˚C for 20 min. The cellular DNA content was measured via EPICS XL flow cytometer (Beckman Coulter, Inc.) at 488 nm excitation wavelength, and the proliferation index (PI) was calculated by FlowJo software (v. 7.6.1; FlowJo LLC), PI=$(S + G_2)/(S + G_2 + G_1)$.

Colony formation assay. Logarithmic growth stage cells (70%) were inoculated into 6-well plates with a microsample gun and cultured in a cell incubator for 10 days. The cell culture fluid was changed every 3 days, and the cell state was closely monitored. Cell colonies were imaged (fluorescence microscope; magnification, x100) before the experiment was terminated. Cells were fixed with 4% paraformaldehyde (Sinopharm Chemical Reagent Co., Ltd.) at room temperature for 30 min and stained with Giemsa solution (Beijing Dingguo Changsheng Biotechnology, Co., Ltd.). The cells were washed and dried repeatedly with ddH_2O. Imaged were captured, and the number of colonies >1 mm were counted.

Migration and invasion assays. Cell invasion and migration assays were performed using Transwell chambers. In the cell migration assay, $1.0x10^5$ transfected cells were inoculated into the upper chamber, and 600 μl 30% FBS-containing medium was added to the lower chamber. The cells were cultured in a 37˚C incubator for 48 h. The non-migrated cells in the chamber were carefully removed with a cotton swab, fixed with 4% paraformaldehyde (Sinopharm Chemical Co., Ltd.) at 37˚C for 15 min and stained with crystal violet (Beyotime Institute of Biotechnology) after drying, following which they were observed and counted under a microscope (light microscope; magnification, x100). For the cell invasion assay, a Matrigel-coated membrane (Becton, Dickinson and Company) was used (pre-coated at 4˚C for 10 min).

Tumorigenicity assays in nude mice. A total of 12 4-week-old male BALB/C nude mice weighing ~20 g were randomly divided into two groups with six mice in each group. Lentiviral-transduced Caco-2 cells (the concentration of cell suspension was $2x10^7$/ml) were subcutaneously injected in nude mice, and the number of cells used per injection was $5x10^5$ cells/mouse. The nude mice were reared at 21±2˚C, relative humidity 30-70%, 12-h light/dark cycle and normal diet. The tumor diameter was measured every 3 days to monitor the growth rate of tumor. The maximum (L) and minimum length (W) of tumor were measured with slide caliper. The tumor volume was calculated using the following formula: Volume = 1/2 (LxW^2) formula. At 28 days after injection, the nude mice were anesthetized with sodium pentobarbital (40 mg/kg) and euthanized via cervical dislocation. The tumors were collected and then weighed. All animal experiments were approved and supervised by the Animal Care Committee of The Fourth Military Medical University (approval no. IACUC-20200402), and were conducted according to international standards for animal welfare (27).

Western blot analysis. Cells were lysed in lysis buffer (Beyotime Institute of Biotechnology). Following centrifugation (4˚C, 13,000 x g, 15 min), the supernatant was collected, and the protein concentration determined using the BCA method (Thermo Fisher Scientific, Inc.). The mass of protein loaded per lane was 20 μg. The protein was separated using 10% SDS-PAGE and transferred to a PVDF membrane (EMD Millipore). After protein transfer and blocking (blocking reagent was TBST solution containing 5% skimmed milk and 0.1% Tween-20), the membrane was incubated with primary antibody (rabbit monoclonal antibody; cat. no. ab130957; Abcam) overnight at 4˚C, and horseradish peroxidase (HRP)-conjugated secondary antibody (1:5,000 dilution, cat. no. 31466; Invitrogen; Thermo Fisher Scientific, Inc.) for 1 h at room temperature and visualized using the ECL reagent (EMD Millipore). GAPDH (mouse monoclonal antibody; cat. no. ab8245; Abcam) and β-actin (rabbit monoclonal antibody; cat. no. SAB5500001; Sigma-Aldrich; Merck KGaA) were used as controls. The bands were measured using an X-ray film and were quantified using ImageJ software (v 1.6.0, NIH).

Immunohistochemistry. The 3 μm thick frozen tissue slices were prepared and rewarmed at room temperature, blocked with 5% goat serum at room temperature for 30 min (Beyotime Institute of Biotechnology) and anti-EI24 antibody (1:200 dilution, cat. no. ab130957; Abcam) was added. The samples were incubated overnight at 4˚C. Sections were then washed with PBS (Gibco; Thermo Fisher Scientific, Inc.), following which the secondary antibody (1:200 dilution; cat. no. 31466; Invitrogen; Thermo Fisher Scientific, Inc.) was added and incubated in a 37˚C incubator for 30 min. Following rinsing with PBS, the tissue microarray was placed in a chromogenic substrate solution (Tiangen Biotech Co., Ltd.) for 10 min and then tap water was used to fully rinse the samples in order to stop the chromogenic process. After 1 min of re-dyeing with hematoxylin at room temperature (Beyotime Institute of Biotechnology), the steps of dehydration, transparency and sealing were conducted, and the results were determined using a microscope (light microscope; magnification, x100).

Tissue microarray immunohistochemical staining. After the aforementioned staining, two pathologists independently interpreted the tissue microarray, including the staining intensity and size of the stained area. The coloring intensity score was as follows: Colorless was scored 0; light yellow scored 1; brown-yellow scored 2; and brown scored 3. The staining
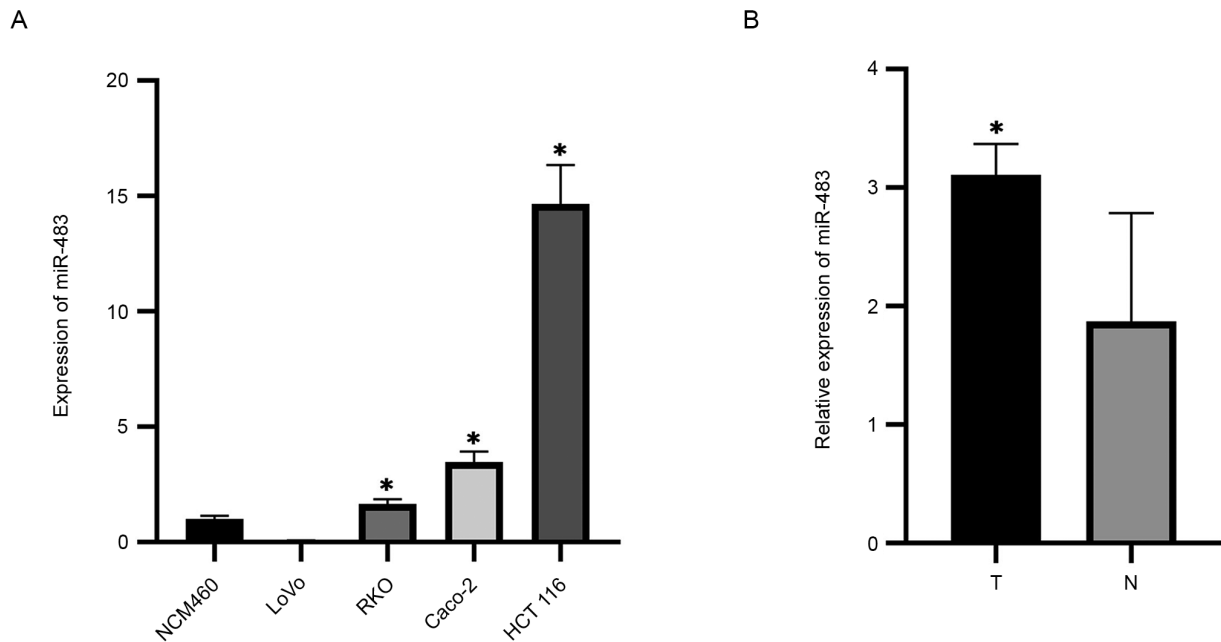
Figure 1. miR-483 is upregulated in CRC tissues and cells. (A) miR-483 expression in CRC cell lines, Caco-2, RKO and HCT 116, was higher than that in normal colorectal gland epithelial cells NCM460, as detected via RT-qPCR. *P<0.05. (B) RT-qPCR results of the relative expression level of miR-483 in CRC paired tissues (T) and adjacent N tissues. *P<0.05 vs. N. CRC, colorectal cancer; RT-qPCR, reverse transcription-quantitative PCR; T, tumor; N, normal; miR, microRNA.

area score was 0 for <5%, 1 for 5-25%, 2 for 26-50%, 3 for 51-75% and 4 for 76-100%. If the scores of the two patholo-gists were different, the average of the two was taken. In this study, the final score of staining intensity was the product of two parts: 0 was negative (-), 1-4 was weak positive (+), 5-8 was positive (++) and 9-12 was strong positive (+++).

Statistical analysis. In the cell experiment, Tukey's post hoc tests and one-way ANOVA were used to compare the differences between the groups. EI24 and miR-483 expression was analyzed using the Wilcoxon signed rank test in CRC tissues and adjacent normal tissues. χ^2 tests were used to analyze the association between the expression level of EI24 and clinical parameters. Kaplan-Meier and logarithmic rank tests were used to compare survival rates, and the Bonferroni correction was applied for pairwise adjustment. Data are presented as mean ± standard deviation. P<0.05 was considered to indicate a statistically significant difference. Triplicate repeats were performed for each experiment. All statistical analyses were performed using SPSS 19.0 software (IBM Corp.).

Results

miR-483 is upregulated in CRC tissues and cells. The current study designed and synthesized specific miRNA primers, and then used RT-qPCR to detect the expression level of miR-483 in CRC cells and corresponding normal colorectal cells. The expression level of miR-483 in the CRC cell lines Caco-2, RKO and HCT 116 was significantly higher compared with that in normal colorectal cells; however, there was no significant difference in its expression in LoVo cells (Fig. 1A). Moreover, the expression level of miR-483 in CRC tissues was signifi-cantly higher compared with in the adjacent normal tissues

(Fig. 1B). Thus, it was suggested that miR-483 may serve a regulatory role in the occurrence and development of CRC.

Overexpression of miR-483 promotes the proliferation, invasion and migration of CRC cells. Caco-2 cell lines with a relatively low expression of miR-483 were selected, and lentivirus expression vectors were used to establish a stable overexpression cell model. The proliferative level of Caco-2 cells in the groups transfected with LV-miR-483 or LV-NC were positive for green immunofluorescence (Fig. 2A). The expression level of miR-483 in these two groups was also detected via RT-PCR. The PCR amplification curves and results revealed that the expression level of miR-483 in the LV-miR-483 transfected Caco-2 cells was significantly higher compared with that in the NC group (Fig. 2A). This observa-tion indicated that LV-miR-483 and LV-NC stable Caco-2 cell lines were successfully established, providing credibility to the subsequent functional experiments.

MTT assay showed that the proliferation of CRC cells was accelerated, leading to greater malignancy (Fig. 2B). Compared with the LV-NC group, the LV-miR-483 group was associated with a lower probability of G1 arrest (Fig. 2C). These results demonstrated that overexpression of miR-483 promoted the proliferation of CRC cells, and participated in the regulation of the cell cycle. Overexpression of miR-483 also increased the proliferation and invasiveness of CRC cells, as shown by colony formation and Transwell assays (Fig. 2D and E). Further experiments revealed that overexpression of miR-483 increased the migration of Caco-2 cells (Fig. 2F), suggesting that miR-483 increased the possibility of distant metastasis of CRC.

In order to further clarify the effect of miR-483 overex-pression on CRC cells, tumorigenicity assays were conducted
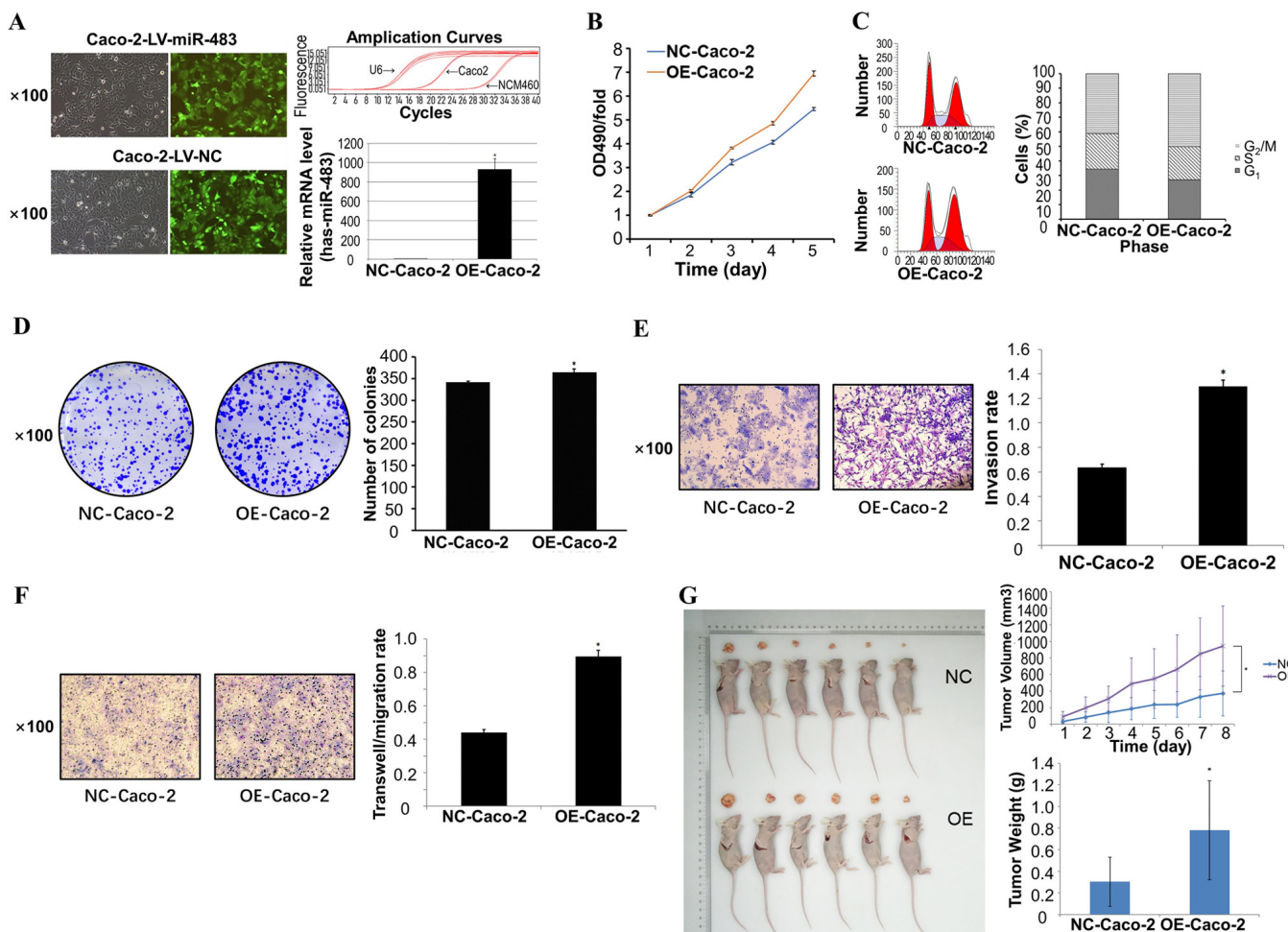
Figure 2. Overexpression of miR-483 promotes the proliferation, invasion and migration of CRC cells. (A) The proliferative level of Caco-2 cells in the two groups transfected with LV-miR-483 and LV-NC was observed by immunofluorescence. The PCR amplification curves and results demonstrated that the expression level of miR-483 in the OE group was significantly higher compared with that in the NC group. (B) MTT assay results revealed that the proliferation rate of the OE group was significantly higher than that of the NC group. (C) Flow cytometry was used to analyze cell cycle and detect the percentage of OE group and NC group cells in G_0/G_1, S and G_2/M phases, suggesting that upregulated miR-483 may be involved in the regulation of the CRC cell cycle. (D) Colony formation assay indicated that the number of cell clones in OE-Caco-2 cells was significantly higher than that in NC group. Transwell (E) invasion and (F) migration assays were used to elucidate the invasion and migration of cells. All error bars represent the SEM of ≥3 independent experiments. The results showed that the mobility and invasive rate of the OE-Caco-2 group were significantly higher than those of NC group. (G) Nude mice tumorigenicity assays detected the effect of miR-483 OE on tumor formation *in vivo*, and the results demonstrated that the tumor volume and tumor weight in the OE group were significantly larger compared with the NC group. *P<0.05 vs. NC-Caco-2. LV-miR-483, miR-483 lentivirus; LV-NC, negative control virus; CRC, colorectal cancer; miR, microRNA; OE, overexpression; OD, optical density.

in nude mice. After subcutaneous implantation of Caco-2 cells in nude mice, tumor volume and weight in the miR-483 overexpression group were significantly higher compared with those in the NC group (Fig. 2G).

EI24 is downregulated in CRC tissues. The RT-qPCR results demonstrated that the expression levels of EI24 in CRC tissues were significantly lower compared with those in adjacent normal tissues (Fig. 3A). The expression intensity of EI24 in cancer and adjacent normal tissues was analyzed using immunohistochemistry, and the results indicated that the expression level of EI24 in adjacent normal tissues was significantly upregulated compared with CRC tissues (Fig. 3B). These experiments suggested that EI24 was weakly expressed in CRC tissues, suggesting that EI24 serves a role as a tumor suppressor gene in CRC and may be a prognostic molecule for CRC.

EI24 expression is associated with patient prognosis. In order to clarify the relationship between the expression level of EI24 and the prognosis of CRC, 183 patients with CRC were recruited. Based on the expression level of EI24 in the immunohistochemical staining of pathological sections, the patients were divided into a high-expression group and a low-expression group. The general data pertaining to the patients are shown in Table SI. Kaplan-Meier and logarithmic rank tests were used for survival analysis. The result demonstrated that there was significant difference between strong positive group (+++) and weak positive group (+; P=0.005), and there was also significant difference between strong positive group (+++) and positive group (++; P=0.03), but there was no significant difference between + and ++ groups (P=0.296). After Bonferroni correction, only +++ and + groups had a significant difference (P<0.05; Fig. 4). The results of the survival analysis indicated that the prognosis of patients with high expression of EI24 was
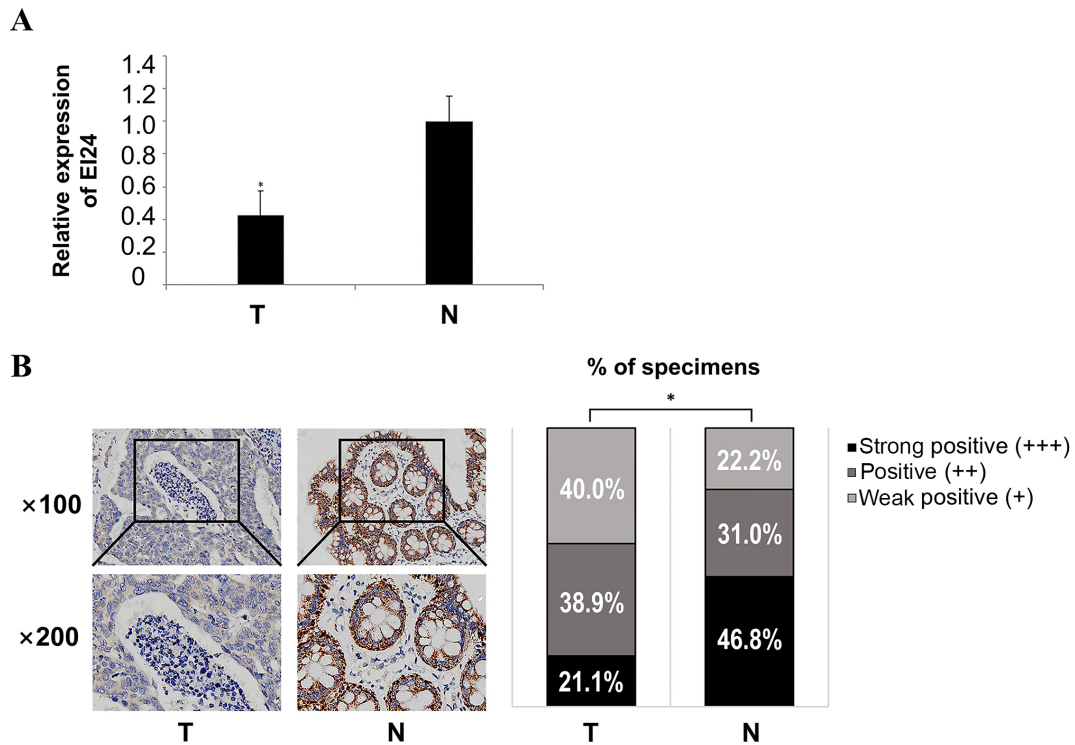
A

B

Figure 3. EI24 is downregulated in CRC tissues. (A) Reverse transcription-quantitative PCR results identified that the expression level of EI24 in CRC tissues (T) was significantly lower than that in adjacent N tissues. *P<0.05 vs. N. (B) The expression level of EI24 in CRC and adjacent N tissues was detected via immunohistochemistry, and the results demonstrated that EI24 expression in adjacent N tissues was significantly higher than that in T tissues. Magnification, x100 and x200. *P<0.05. CRC, colorectal cancer; EI24, EI24 autophagy associated transmembrane protein; T, tumor; N, normal.
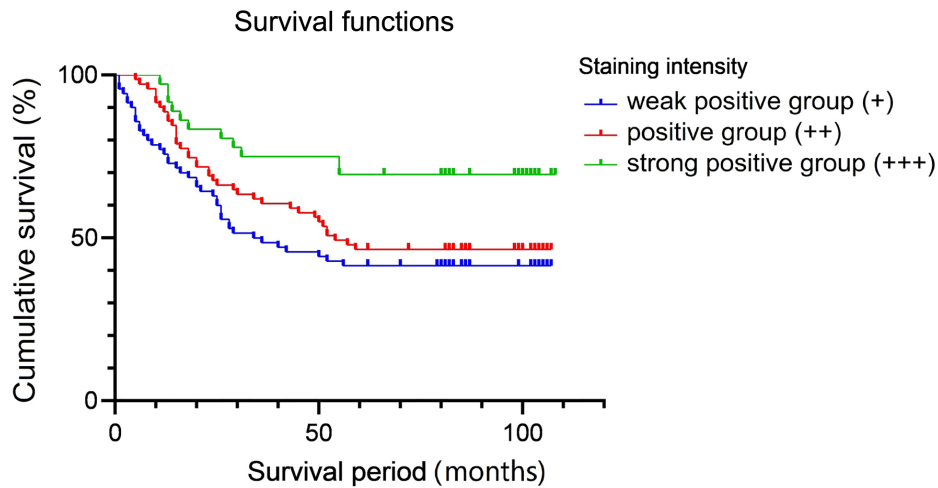

Figure 4. EI24 expression is associated with the prognosis of patients. The clinical and pathological data of 183 patients with CRC were collected. According to the expression of EI24 in immunohistochemical staining, the patients were divided into weak positive group (+), positive group (++) and strong positive group (+++). Survival curves were drawn according to the follow-up results of the groups. Survival analysis showed that strong positive group (+++) was significantly different from the weak positive group (+) (P=0.005), and there was also significant difference between strong positive group (+++) and positive group (++) (P=0.03), but there was no significant difference between + and ++ groups (P=0.296). After Bonferroni correction, only +++ and + groups had a significant difference (P<0.05). Survival analysis showed that the survival time of patients with high expression of EI24 was significantly increased compared with that of patients with low expression of EI24. EI24, EI24 autophagy associated transmembrane protein.

improved compared with that of patients with a low expression of EI24.

miR-483 expression is negatively associated with EI24 levels in CRC tissues. Our previous studies reported that the expression level of miR-483 was increased in esophageal squamous cell

carcinoma, and that upregulation of miR-483 could promote the development of esophageal cancer (24,28). Furthermore, a reporter gene test confirmed that EI24 was the target molecule of miR-483 (21). In the current experiment, the expression level of EI24 in miR-483 overexpressing stable Caco-2 cells and in the NC group was detected using RT-qPCR. It was found
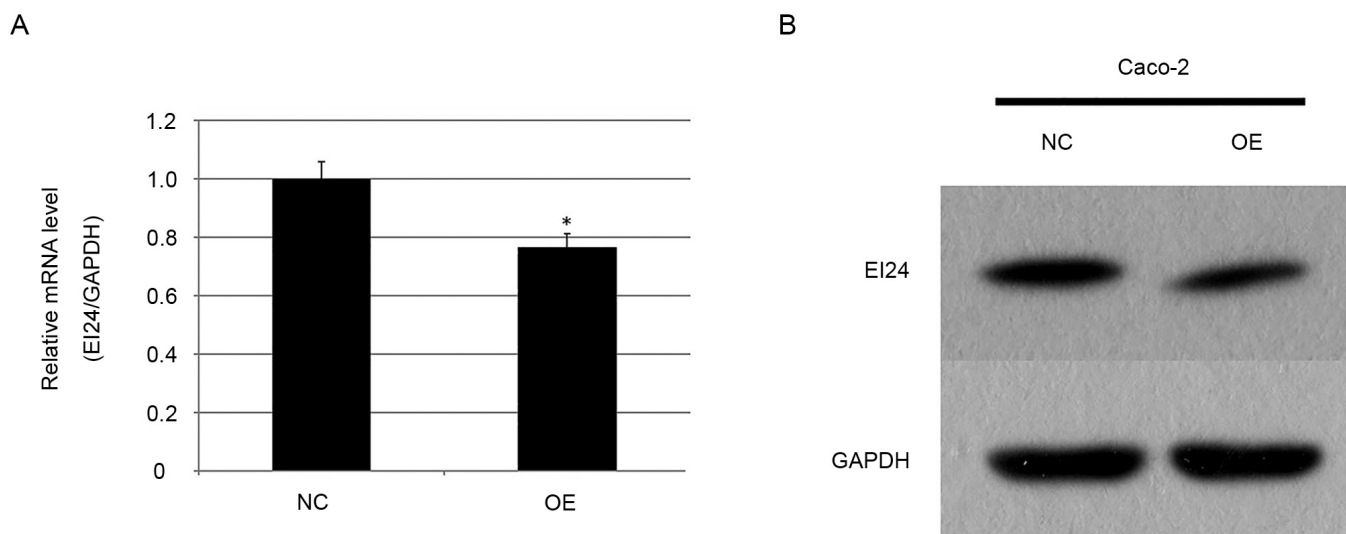
A

B

Figure 5. Negative correlation of miR-483 and EI24 expression in CRC cell lines. (A) Reverse transcription-quantitative PCR results of the expression level of EI24 in Caco-2 cells overexpressing miR-483. The results demonstrated that the expression abundance of EI24 gene in CRC cells was 76.6% of that in the NC group. *P<0.05 vs. NC. (B) Western blotting was used to detect the expression level of EI24 in Caco-2 cells overexpressing miR-483. The results indicated that the expression level of EI24 was significantly lower compared with that of the NC, suggesting that overexpression of miR-483 may inhibit EI24 protein expression. EI24, EI24 autophagy associated transmembrane protein; NC, negative control; miR, microRNA; OE, overexpression.

that the expression level of EI24 in the overexpression group was 0.766 times higher compared with that in the NC group (P<0.05; Fig. 5A). Western blotting was also used to detect the expression level of EI24 in the miR-483 overexpressing CRC cell line (Fig. 5B), and it was identified that EI24 expression in the overexpression group was notably lower compared with that in the NC group, suggesting that upregulation of miR-483 may inhibit the expression of EI24 protein. These results are consistent with our previous studies (24,28), suggesting a targeting relationship between miR-483 and EI24.

Endogenous miR-483 modulates EI24 expression and CRC cell proliferation. To investigate whether endogenous miR-483 regulates EI24 expression, the effect of an miR-483 inhibitor in Caco-2 cells, which relatively expresses high levels of miR-483, was determined. miR-483 inhibitor (cat. no. miR20002173-1-5; Guangzhou RiboBio Co., Ltd.) and the NC (cat. no. miR20002173-1-5; Guangzhou RiboBio Co., Ltd.) were used for this experiment. Compared with the NC group, the expression level of miR-483 was significantly decreased in the cells transfected with inhibitor (Fig. 6A). Furthermore, the transfection of the miR-483 inhibitor markedly enhanced EI24 expression both at the mRNA and protein levels (Fig. 6B and C). Moreover, CRC cell proliferation was significantly increased after miR-483 inhibitor transfection (Fig. 6D). These findings may suggest that miR-483 endogenously modulates EI24 expression and CRC cell proliferation.

Discussion

Invasion and metastasis are important characteristics of CRC and are one of the main causes of mortality in patients with CRC (1). The invasion and proliferation of cancer cells are continuous and dynamic biological processes involving multiple steps and factors (29). The process consists of several relatively independent steps, including separation and exfoliation of cancer cells, adhesion between cancer cells and the cell matrix, invasion and movement of cancer cells, invasion and penetration of vascular walls, the presence and survival of cancer cells in the circulatory system, penetration of the hemorrhagic wall by cancer cells, implantation of cancer cells in distal organs, and the proliferation and metastasis of cancer cells after neovascularization (30). Although a variety of CRC-related molecules have been identified, the signal regulatory networks involved in the invasion and metastasis of CRC are complex, and the specific mechanisms, molecular markers and targets of action remain to be fully determined. Therefore, it is important to investigate the key molecules and molecular mechanisms of CRC metastasis, and to identify effective intervention targets. Current studies have shown that the mechanisms of CRC metastasis involve the epithelial-mesenchymal transformation (EMT)-related signaling pathway, Wnt/β-catenin signaling pathway, Notch signaling pathway, TGF-β signaling pathway, tumor-related genes, including p53, and numerous miRNA molecules (31-36).

Invasive and metastatic behaviors are important biological features of malignant tumors and are also important factors leading to the progression of tumors and the outcome of treatment (37). The invasion and metastasis of tumors are a dynamic process, involving the interaction of multiple factors associated with the tumor cells themselves, and are also closely related to their microenvironment, forming complex signaling pathways (38). A large number of studies have reported that miR-483 was involved in the invasion and metastasis of tumors. For instance, a study on esophageal cancer showed that miR-483-5p was positively correlated with lymph node metastasis of esophageal cancer (39). In addition to the digestive system, a study of lung cancer suggested that miR-483-5p was activated by the Wnt/β-catenin signaling pathway, and promoted metastasis by directly acting on two metastasis inhibitors, GDP dissociation inhibitor 1 (RhoGDI1) and activated leukocyte adhesion molecule (ALCAM). The
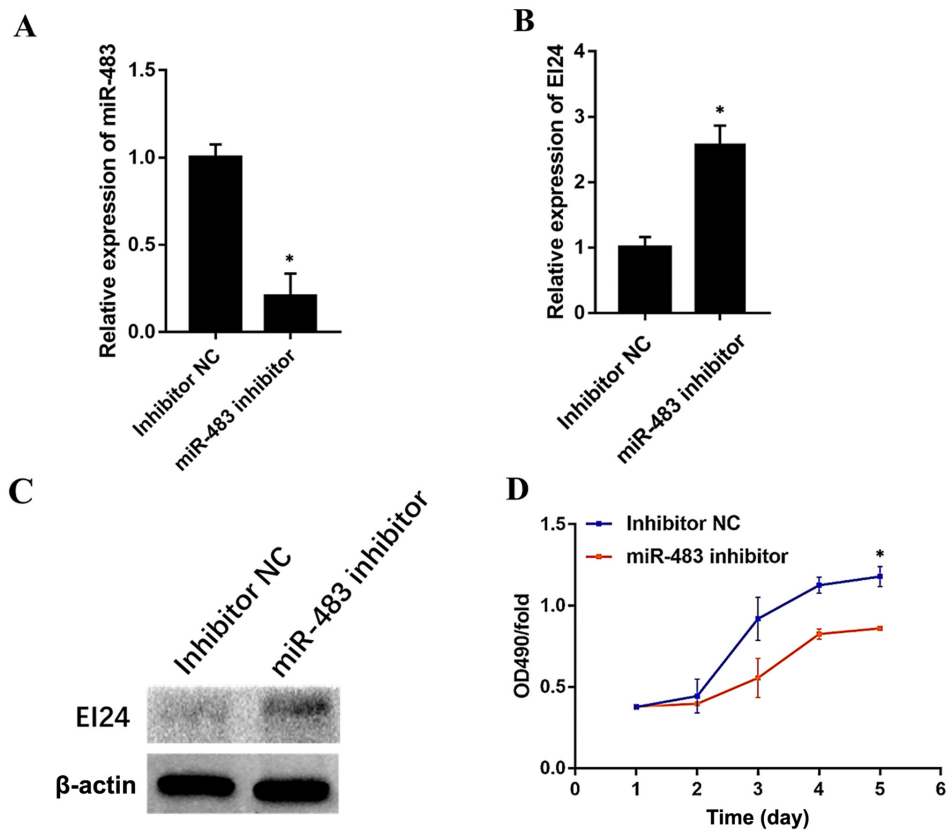
Figure 6. Endogenous miR-483 modulates EI24 expression and CRC cell proliferation. (A) RT-qPCR was used to detect the expression level of miR-483 after transfection of miR-483 inhibitor in Caco-2 cells. The results showed that miR-483 expression was significantly decreased in the inhibitor group. (B) RT-qPCR was used to detect the expression level of EI24 in Caco-2 cells transfected with miR-483 inhibitor. The results demonstrated that EI24 gene expression in the miR-483 inhibitor group was 2.584 times higher compared with that in the NC group. *$P<0.05$ vs. inhibitor NC. (C) Western blot analysis was used to detect the expression level of EI24 in Caco-2 cells with miR-483 knockdown. The results indicated that EI24 protein expression was markedly higher compared that of the NC group, further suggesting that miR-483 may inhibit the expression of EI24 protein. (D) MTT assay results showed that the proliferative rate of the miR-483 inhibitor group was significantly lower compared with that of the NC group. *$P<0.05$ vs. inhibitor NC. EI24, EI24 autophagy associated transmembrane protein; NC, negative control; miR, microRNA; RT-qPCR, reverse transcription-quantitative PCR; OD, optical density.

downregulation of RhoGDI1 can enhance snail family transcriptional repressor 1 gene expression, thereby promoting the EMT (14,40). Moreover, the expression level of miR-483-5p was positively correlated with the expression level of the β-catenin protein but was negatively correlated with the expression levels of RhoGDI1 and ALCAM. Therefore, miR-483-5p was not only the key factor involved in activating β-catenin to promote metastasis but was also a negative regulator of the metastasis inhibitors RhoGDI1 and ALCAM (14). The present results demonstrated that miR-483 was highly expressed in CRC cells. *In vivo* and *in vitro* experiments revealed that miR-483 served a regulatory role in the proliferation of CRC cells, and overexpression of miR-483 promoted the invasion and migration of CRC cells. After completing the current study, additional MTT assay, plate colony formation assay, Transwell invasion experiment, cell cycle assay and nude mouse tumorigenesis tests were performed in an RKO cell line, and the results were consistent with those of Caco-2 cell line (data not shown).

EI24 is downregulated in malignant tumors of the digestive tract, including pancreatic ductal adenocarcinoma and esophageal cancer, as well as in breast, lung and skin cancer types (24). Zang *et al* (18) reported that the mRNA expression level of EI24 in pancreatic ductal adenocarcinoma tissue was downregulated compared with adjacent normal tissues, and the downregulation trend was associated with the degree of differentiation of cancer cells. Furthermore, overexpression of EI24 reduced the expression level of the oncogene c-Myc by activating c-Myc autophagic lysosomes, thereby inhibiting the proliferation of cancer cells and promoting cell cycle stagnation. Thus, these authors proposed the hypothesis that the EI24/Beclin-1/p62/c-Myc pathway mediated the progression of pancreatic ductal adenocarcinoma, and it was suggested that EI24 served an important role in anti-oncogenesis (18). Moreover, Li *et al* (19) revealed that the expression level of miR-455-3p was increased in triple negative breast cancer, which promoted the proliferation, invasion and migration of cancer cells. The authors further predicted, and verified, that EI24 was a target gene. In addition, it was found the knockdown of EI24 expression using small interfering RNA could enhance the invasion and migration of cancer cells, and miR-455-3p could enhance the invasion and migration of cancer cells. Thus, targeting the tumor suppressor gene EI24 promoted the invasion and migration of tumors (19). The aforementioned studies showed that EI24 expression was significantly decreased in tumor tissues, potentially inhibiting the occurrence and metastasis of tumors. In the present study, it was identified that the expression level of EI24 in CRC tissues was lower compared

with that in adjacent normal tissues. Moreover, the survival analysis of CRC patients revealed that patients with high EI24 expression had a n improved prognosis.

Both miR-483 and EI24 are involved in important biological processes, including tumor cell proliferation, invasion and migration, and they overlap in the process of tumor metastasis (28). Our previous study revealed that the expression level of miR-483 was increased in esophageal cancer (24). Furthermore, upregulation of miR-483 promotes cancer cell proliferation, migration and other malignant phenotypes, whereas downregulation of miR-483 could inhibit malignant phenotypes (41). These results suggested that miR-483 could serve a role in promoting esophageal cancer. Bioinformatics analyses and genome-wide expression profile chips were combined to predict that EI24 may be the downstream target gene of miR-483, and that miR-483 may promote the metastasis and progression of cancer cells by inhibiting the expression of EI24 (24). Therefore, miR-483 may promote the metastasis of CRC by regulating the expression level of EI24. The present study conducted experiments using RT-qPCR and western blotting. These experiments demonstrated that miR-483 could inhibit the expression level of EI24, which suggested the existence of a miR-483/EI24 signaling pathway. miR-483 appears to be co-expressed with its host gene IGF2 and promote the proliferation of CRC cells by inhibiting its downstream target gene DLC-1 (42). These results suggest that the miR-483/EI24 signaling pathway may serve an important role in the metastasis of CRC, representing a possible alternative for the future treatment of CRC.

There were several limitations to the current study. Recent studies have reported that the occurrence and progression of CRC are associated a series of oncogenes and tumor suppressor gene mutations, including RAS, BRAF, PIK3CA and TP53 gene, amongst others (40,43,44). However, such tests were not performed at this time. Therefore, future studies will detect and analyze the expression of related genes in CRC with abnormal expression of miR-483. In addition, relevant experiments will be performed in other CRC cell lines, to obtain more complete results. Overexpression and gene knockout tests should also be performed to assess the intrinsic association between miR-483 and EI24. The sample size of clinical data should be expanded, and patient-related genetic testing results should be collected. Further studies should focus on the investigation of the upstream and downstream pathways of miR-483, and the mechanisms via which miR-483 regulates the cellular proliferation and metastasis of CRC.

In conclusion, the present study demonstrated that miR-483 could regulate the expression level of EI24 by targeting EI24, as well as promoted the proliferation, migration and invasion of CRC cells.

Acknowledgements

Availability of data and materials

The datasets used and/or analyzed during the current study are available from the corresponding author on reasonable request.

Authors' contributions

WZ and HZ are responsible for confirming the authenticity of the raw data. WZ, WY, JY and HZ participated in the design and performance of the experiments. LD, XW and YL contributed to the data analysis. LN, SX and RZ contributed to the collection of samples and clinical data analyses. JY and LH participated in the conception and design of manuscripts, coordinated the acquisition of clinical specimens and interpretated the data results. All authors read and approved the final manuscript, and agree to be accountable for all aspects of the research in ensuring that the accuracy or integrity of any part of the work are appropriately investigated and resolved.

Ethics approval and consent to participate

All procedures performed in the present study involving human participants were approved by the Ethic Committee of Xijing Hospital of The Fourth Military Medical University/Air Force Military Medical University (Xi'an, China; approval no. KY20203211-1). Written informed consent for the publication of any associated data and accompanying images was obtained from all patients prior to surgery. All animal experiments were approved and supervised by the Animal Care Committee of The Fourth Military Medical University (approval no. IACUC-20200402), according to international standards for animal welfare.

Patient consent for publication

Not applicable.

Competing interests

The authors declare that they have no competing interests.

References

1. Dekker E, Tanis PJ, Vleugels JLA, Kasi PM and Wallace MB: Colorectal cancer. Lancet 394: 1467-1480, 2019.
2. Yang Q, Hou C, Huang D, Zhuang C, Jiang W, Geng Z, Wang X and Hu L: miR-455-5p functions as a potential oncogene by targeting galectin-9 in colon cancer. Oncol Lett 13: 1958-1964, 2017.
3. Brenner H, Kloor M and Pox CP: Colorectal cancer. Lancet 383: 1490-1502, 2014.
4. Zhou W, Zhou X, Liu JQ, Zhang YJ and Hong L: High expression of miR-21 in tissue correlated with the poor survival of patients with esophageal cancer: A pilot study using the meta-analysis. J Prev Med Care 1: 9-15, 2016.
5. Chen X, Zhang DH and You ZH: A heterogeneous label propagation approach to explore the potential associations between miRNA and disease. J Transl Med 16: 348, 2018.
6. Ma J, Hong L, Chen Z, Nie Y and Fan D: Epigenetic regulation of microRNAs in gastric cancer. Dig Dis Sci 59: 716-723, 2014.
7. Chi SW, Zang JB, Mele A and Darnell RB: Argonaute HITS-CLIP decodes microRNA-mRNA interaction maps. Nature 460: 479-486, 2009.
8. Zhou W, Yang W, Ma J, Zhang H, Li Z, Zhang L, Liu J, Han Z, Wang H and Hong L: Role of miR-483 in digestive tract cancers: From basic research to clinical value. J Cancer 9: 407-414, 2018.

9. Ferland-McCollough D, Fernandez-Twinn DS, Cannell IG, David H, Warner M, Vaag AA, Bork-Jensen J, Brøns C, Gant TW, Willis AE, *et al*: Programming of adipose tissue miR-483-3p and GDF-3 expression by maternal diet in type 2 diabetes. Cell Death Differ 19: 1003-1012, 2012.

10. Wang H, Zhang H, Sun Q, Wang Y, Yang J, Yang J, Zhang T, Luo S, Wang L, Jiang Y, *et al*: Intra-articular delivery of Antago-miR-483-5p inhibits osteoarthritis by modulating matrilin 3 and tissue inhibitor of metalloproteinase 2. Mol Ther 25: 715-727, 2017.

11. Qiao Y, Ma N, Wang X, Hui Y, Li F, Xiang Y, Zhou J, Zou C, Jin J, Lv G, *et al*: miR-483-5p controls angiogenesis in vitro and targets serum response factor. FEBS Lett 585: 3095-3100, 2011.

12. Shi L, Liu S, Zhao WQ and Shi JZ: miR-483-5p and miR-486-5p are down-regulated in cumulus cells of metaphase II oocytes from women with polycystic ovary syndrome. Reprod Biomed Online 31: 565-572, 2015.

13. Yu X, Li Z, Chan MT and Wu WK: The roles of microRNAs in Wilms' tumors. Tumour Biol 37: 1445-1450, 2016.

14. Song Q, Xu Y, Yang C, Chen Z, Jia C, Chen J, Zhang Y, Lai P, Fan X, Zhou X, *et al*: miR-483-5p promotes invasion and metastasis of lung adenocarcinoma by targeting RhoGDI1 and ALCAM. Cancer Res 74: 3031-3042, 2014.

15. Patterson EE, Holloway AK, Weng J, Fojo T and Kebebew E: MicroRNA profiling of adrenocortical tumors reveals miR-483 as a marker of malignancy. Cancer 117: 1630-1639, 2011.

16. Si Y, Zhang H, Ning T, Bai M, Wang Y, Yang H, Wang X, Li J, Ying G and Ba Y: miR-26a/b inhibit tumor growth and angiogenesis by targeting the HGF-VEGF axis in gastric carcinoma. Cell Physiol Biochem 42: 1670-1683, 2017.

17. Xue L, Nan J, Dong L, Zhang C, Li H, Na R, He H and Wang Y: Upregulated miR-483-5p expression as a prognostic biomarker for esophageal squamous cell carcinoma. Cancer Biomark 19: 193-197, 2017.

18. Zang Y, Zhu L, Li T, Wang Q, Li J, Qian Y, Wei L, Xie M, Tang WH, Liu X, *et al*: EI24 suppresses tumorigenesis in pancreatic cancer via regulating c-Myc. Gastroenterol Res Pract 2018: 2626545, 2018.

19. Li Z, Meng Q, Pan A, Wu X and Li L: MicroRNA-455-3p promotes invasion and migration in triple negative breast cancer by targeting tumor suppressor EI24. Oncotarget 8: 19455-19466, 2017.

20. Choi JM, Jang JY, Choi YR, Kim HR, Cho BC and Lee HW: Reduced expression of EI24 confers resistance to gefitinib through IGF-1R signaling in PC9 NSCLC cells. Lung Cancer 90: 175-181, 2015.

21. Nam TW, Park SY, Lee JH, Roh JI and Lee HW: Effect of EI24 expression on the tumorigenesis of Apc[Min/+] colorectal cancer mouse model. Biochem Biophys Res Commun 514: 1087-1092, 2019.

22. Choi JM, Devkota S, Sung YH and Lee HW: EI24 regulates epithelial-to-mesenchymal transition and tumor progression by suppressing TRAF2-mediated NF-κB activity. Oncotarget 4: 2383-2396, 2013.

23. Mazumder Indra D, Mitra S, Singh RK, Dutta S, Roy A, Mondal RK, Basu PS, Roychoudhury S and Panda CK: Inactivation of CHEK1 and EI24 is associated with the development of invasive cervical carcinoma: Clinical and prognostic implications. Int J Cancer 129: 1859-1871, 2011.

24. Ma J, Hong L, Xu G, Hao J, Wang R, Guo H, Liu J, Zhang Y, Nie Y and Fan D: miR-483-3p plays an oncogenic role in esophageal squamous cell carcinoma by targeting tumor suppressor EI24. Cell Biol Int 40: 448-455, 2016.

25. Mentz RJ, Hernandez AF, Berdan LG, Rorick T, O'Brien EC, Ibarra JC, Curtis LH and Peterson ED: Good clinical practice guidance and pragmatic clinical trials: Balancing the best of both worlds. Circulation 133: 872-880, 2016.

26. Livak KJ and Schmittgen TD: Analysis of relative gene expression data using real-time quantitative PCR and the 2(-Delta Delta C(T) method. Methods 25: 402-408, 2001.

27. MacArthur Clark JA and Sun D: Guidelines for the ethical review of laboratory animal welfare People's Republic of China National Standard GB/T 3589218 [Issued 6 February 2018 Effective from 1 September 2018]. Animal Model Exp Med 3: 103-113, 2020.

28. Duan L, Ma J, Yang W, Cao L, Wang X, Niu L, Li Y, Zhou W, Zhang Y, Liu J, *et al*: EI24 inhibits cell proliferation and drug resistance of esophageal squamous cell carcinoma. Front Oncol 10: 1570, 2020.

29. Malki A, ElRuz RA, Gupta I, Allouch A, Vranic S and Al Moustafa AE: Molecular mechanisms of colon cancer progression and metastasis: Recent insights and advancements. Int J Mol Sci 22: 130, 2020.

30. Leber MF and Efferth T: Molecular principles of cancer invasion and metastasis (review). Int J Oncol 34: 881-895, 2009.

31. Vu T and Datta PK: Regulation of EMT in colorectal cancer: A culprit in metastasis. Cancers (Basel) 9: 171, 2017.

32. Haase G, Gavert N, Brabletz T and Ben-Ze'ev A: The Wnt target gene L1 in colon cancer invasion and metastasis. Cancers (Basel) 8: 48, 2016.

33. Weidle UH, Birzele F and Krüger A: Molecular targets and pathways involved in liver metastasis of colorectal cancer. Clin Exp Metastasis 32: 623-635, 2015.

34. Liu X, Ji Q, Fan Z and Li Q: Cellular signaling pathways implicated in metastasis of colorectal cancer and the associated targeted agents. Future Oncol 11: 2911-2922, 2015.

35. Huang D, Sun W, Zhou Y, Li P, Chen F, Chen H, Xia D, Xu E, Lai M, Wu Y and Zhang H: Mutations of key driver genes in colorectal cancer progression and metastasis. Cancer Metastasis Rev 37: 173-187, 2018.

36. Huang S, Tan X, Huang Z, Chen Z, Lin P and Fu SW: MicroRNA biomarkers in colorectal cancer liver metastasis. J Cancer 9: 3867-3873, 2018.

37. Niu L, Yang W, Duan L, Wang X, Li Y, Xu C, Liu C, Zhang Y, Zhou W, Liu J, *et al*: Biological implications and clinical potential of metastasis-related miRNA in colorectal cancer. Mol Ther Nucleic Acids 23: 42-54, 2020.

38. Allgayer H, Leupold JH and Patil N: Defining the 'Metastasome': Perspectives from the genome and molecular landscape in colorectal cancer for metastasis evolution and clinical consequences. Semin Cancer Biol 60: 1-13, 2020.

39. Zhou Y and Hong L: Prediction value of miR-483 and miR-214 in prognosis and multidrug resistance of esophageal squamous cell carcinoma. Genet Test Mol Biomarkers 17: 470-474, 2013.

40. Wang C, Wang X, Su Z, Fei H, Liu X and Pan Q: miR-25 promotes hepatocellular carcinoma cell growth, migration and invasion by inhibiting RhoGDI1. Oncotarget 6: 36231-36244, 2015.

41. Xiao Y, Guo Q, Jiang TJ, Yuan Y, Yang L, Wang GW and Xiao WF: miR-483-3p regulates osteogenic differentiation of bone marrow mesenchymal stem cells by targeting STAT1. Mol Med Rep 20: 4558-4566, 2019.

42. Cui H, Liu Y, Jiang J, Liu Y, Yang Z, Wu S, Cao W, Cui IH and Yu C: IGF2-derived miR-483 mediated oncofunction by suppressing DLC-1 and associated with colorectal cancer. Oncotarget 7: 48456-48466, 2016.

43. Løes IM, Immervoll H, Sorbye H, Angelsen JH, Horn A, Knappskog S and Lønning PE: Impact of KRAS, BRAF, PIK3CA, TP53 status and intraindividual mutation heterogeneity on outcome after liver resection for colorectal cancer metastases. Int J Cancer 139: 647-656, 2016.

44. Kawaguchi Y, Kopetz S, Newhook TE, De Bellis M, Chun YS, Tzeng CD, Aloia TA and Vauthey JN: Mutation status of RAS, TP53, and SMAD4 is superior to mutation status of RAS alone for predicting prognosis after resection of colorectal liver metastases. Clin Cancer Res 25: 5843-5851, 2019.